Vol. 04, Iss. 2 (2026) 176-187, DOI: 10.61552/JME.2026.02.005

JME

Journal of Materials and Engineering

www.jme.aspur.rs

Exploratory Study on the Wear Behavior of AISI 4140 Steel under Starved Lubrication and Laser Surface Texturing Conditions

Juan Carlos Cervantes[a,*]

[a]*School of Engineering and Technology, University of Monterrey, San Pedro Garza Garcia, Mexico.*

Keywords:

AISI 4140 steel
Wear
Starved lubrication
Laser surface texturing
Block-on-Ring

* Corresponding author:

Juan Carlos Cervantes
E-mail: juan.cervantesm@udem.edu

Received: 12 February 2026
Revised: 16 March 2026
Accepted: 28 April 2026

A B S T R A C T

Wear in steel-to-steel contact systems represents a critical challenge under limited lubrication conditions. This study presents an exploratory investigation of the wear behavior of AISI 4140 steel in contact with D2 steel under starved lubrication and laser surface texturing conditions. A block-on-ring configuration was used to simulate sliding contact. A commercial water-based cutting fluid with emulsified characteristics was applied under starved conditions. Unlike conventional approaches favoring smaller texture diameters and high texture densities to promote uniform lubricant distribution, in this study a laser surface texturing was implemented using larger circular pattern designed to enhance lubricant retention under starved lubrication regime. The results show a consistent trend toward reduced wear and improved friction stability when starved lubrication and the proposed surface texturing are combined allowing to reduce wear (mass lost) by 90% and significantly reducing the coefficient of friction by 73% compared to the maximum value observed in dry conditions. Surface observations suggest that the textured features promote lubricant retention and debris entrapment under boundary lubrication regimes. Although no statistical analysis was performed, the findings provide relevant insights into wear mitigation strategies under constrained lubrication conditions. Overall, the results highlight the importance of texture volumetric capacity in starved lubrication regimes.

1. INTRODUCTION

Wear significantly affects the performance and durability of mechanical systems involving sliding contact [1]. In steel-to-steel interfaces, insufficient lubrication leads to direct asperity interaction, promoting adhesive and abrasive wear mechanisms [2].

Under boundary lubrication conditions, the lubricant film is not sufficient to fully separate contacting surfaces, resulting in increased friction and material degradation [2]. Therefore, improving tribological performance under such conditions remains a key engineering challenge.

Laser surface texturing (LST) has been widely investigated as a technique to enhance tribological behavior by modifying surface topography [3-6]. Textured surfaces can act as micro-reservoirs for lubricant retention and as traps for wear debris, reducing third-body abrasion and improving frictional response.

Conventional approaches in LST design typically favor small texture diameters and high texture densities to promote uniform lubricant distribution [3, 4]. However, under starved lubrication conditions, where lubricant availability is limited, the volumetric capacity of surface features may play a more significant role than distribution alone [7, 8].

Water-based emulsified fluids, such as the one used in this study, are commonly employed not only in machining processes but also in other metalworking and tribological applications where cooling, lubrication, and debris removal are required [9]. Therefore, understanding their behavior under limited lubrication conditions is relevant for a broad range of industrial systems.

Despite extensive research on LST, the combined effect of surface texturing and starved lubrication on AISI 4140 steel in contact with D2 steel remains insufficiently explored. This study aims to provide an exploratory evaluation of this interaction using controlled experimental conditions.

2. EXPERIMENTAL METHOD

The tribological system consisted of AISI 4140 steel conformal blocks in contact with D2 steel rings using a block-on-ring configuration in accordance with ASTM G77-05 [10].

The tests were executed using a T05 Block-on-Ring Wear Tester manufactured by the Institute for Sustainable Technologies National Research Institute RADOM shown in Fig. 1.

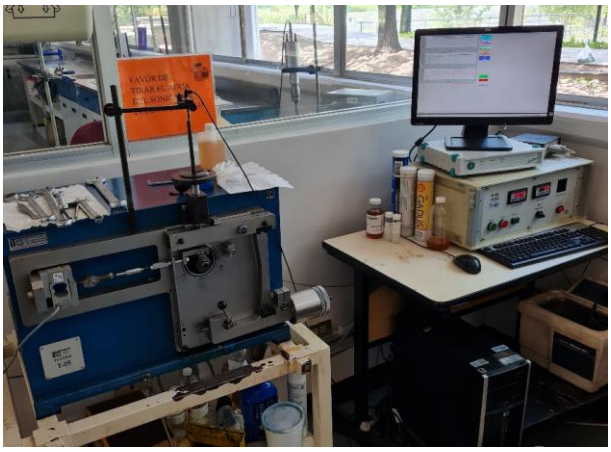

Fig. 1. T05 Block-on-Ring Wear Tester machine used for the testing.

2.1 Test conditions

Experiments were conducted under the parameters shown in Table 1:

Table 1. T05 test parameters.

T05 parameters	Value	Units
Normal Load	0.5	Kg
Rotational speed	400	RPM
Test duration	3,600	Seconds
Temperature	~36	ºC

No active laboratory temperature control was implemented.

2.2 Experimental design

A reduced factorial design (2^2) was used to evaluate:

- Factor A: Starved lubrication.
- Factor B: Laser surface texturing.

Limited replication (2 replicates per experiment) was performed due to the exploratory nature of the study as well as due to time and resources constraints. The combinations of the design are shown in Table 2.

Table 2. DoE set-up.

Experiment	Factors		Combination
	A (lubrication)	B (LST)	
1	-	-	1
2	+	-	A
3	-	+	B
4	+	+	AB

2.3 Lubrication condition

A commercial water-based cutting fluid with emulsified appearance was used. The lubricant exhibited a milky-brown coloration, consistent with semi-synthetic fluids commonly employed in machining operations.

Starved lubrication conditions were simulated by limiting lubricant availability without replenishment, promoting boundary lubrication behaviour [2].

2.4 Laser surface texturing

Several authors have explored the benefits of different laser surface textures involving a wide variety of patterns, shapes, arrays, and lubrication conditions [3-5, 11, 12].

Unlike conventional designs, in this study a relatively larger texture diameter was selected to increase volumetric capacity for lubricant retention and debris entrapment.

The laser surface texturing pattern was design using EzCad2 software, version 2-14-10. A circular hatch pattern with a radius of 0.5mm was chosen for this study.

Laser surface texturing was applied using a Dincel Laser Marking Machine to create a circular hatch pattern. The laser mark was applied at 90º (with respect to ground) on the concave surface that is in contact with the D2 ring as shown in Fig. 2.

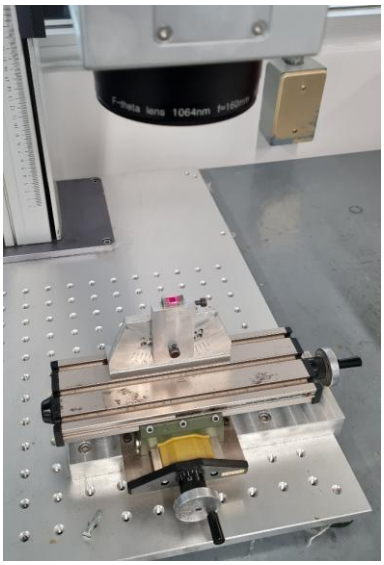

Fig. 2. Laser surface marking area on 4140T block samples.

The process parameters included controlled laser power, frequency, and scanning speed as shown in Table 3. After texturing, samples were polished to remove oxides while preserving surface features.

Table 3. LST parameters.

LST Parameters	Value	Units
Array type	rectangle	-
Array in X axis	10	-
Array in Y axis	10	-
Array X distance	0.1	mm
Array Y distance	0.1	mm
Loop count	3	-
Speed	400	mm/second
Power	100	%
Frequency	20	kHz

After the LST process, the concave surface of the block was polished using an A-99 500 sandpaper to remove the residual material that was displaced by the laser due to the heating applied on the surface to form the circular cavities as well as the oxides generated by the interaction between the laser and the 4140T steel as shown in Fig. 3.

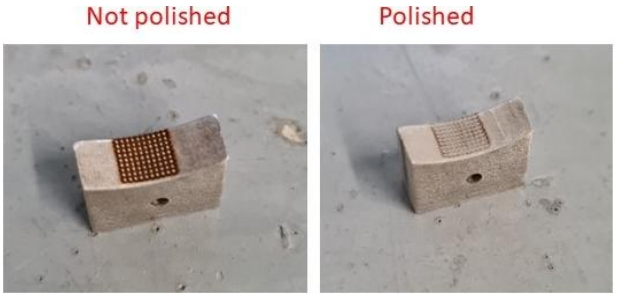

Fig. 3. LST finish surface after polishing the AISI 4140 block samples.

After the polishing process, the blocks were weighted in the analytical balance to take into consideration the mass of material that was removed in the polishing process and then obtain the weigh reference to evaluate the wear rate after completing the T05 test for the effects B and AB.

2.5 Wear evaluation

Wear performance was evaluated through:

- Mass loss measurements using a A&D Phoenix GH-120 analytical balance.
- Coefficient of Friction behaviour (COF).
- Surface morphology analysis using a 3D optical scanning: Bruker Alicona optical scanner.

3. RESULTS

In this section the results of each of the combinations are presented. Then the discussion and analysis of the results will be presented.

3.1 Surface morphology

Surface analysis using the Alicona system revealed distinct wear patterns:

3.2 Combination 1

Combination 1 involved executing the test without any lubrication nor LST. As it is shown in Fig. 4 the average displacement increased up to 31.4375 µm at the end of the test. The frictional force reached a maximum value of 5.61 N and showed a stabilized decreasing tendency below this value.

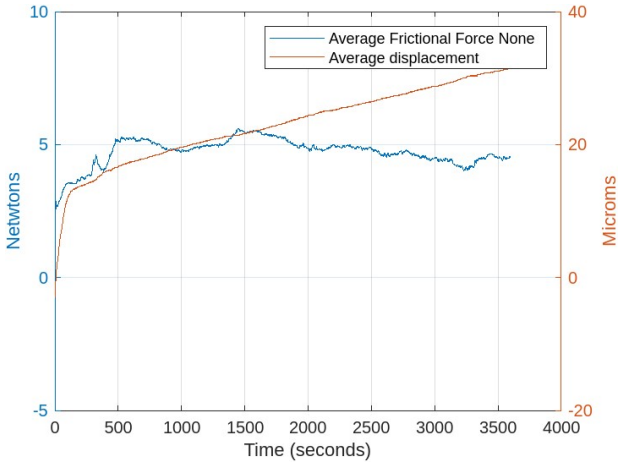

Fig. 4. Average frictional force and displacement versus time for combination 1.

After the test, the 4140T block samples were analysed in the Bruker Alicona optical scanner as shown in Fig. 5

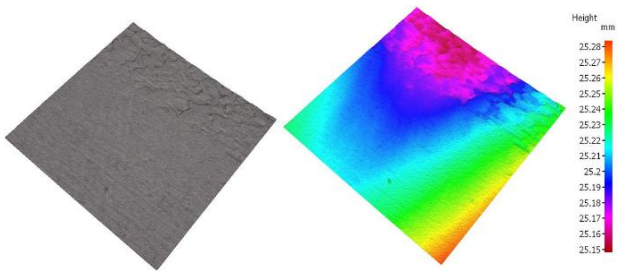

Fig. 5. 3D scanned image of work area from a sample of combination 1.

The 3D image of one of the samples shows that the 4140T block surface that was in frictional contact with the D2 ring presents a polished surface due to material displacement.

The samples were weighted in the A&D Phoenix GH-120 analytical balance. The average weight of the 4140T block samples before the wear test was of 7.47435 grams. After the test, the average mass of 4140T steel lost was of 0.00105 g. This shows that the average material lost due to frictional contact without lubrication or LST was of 0.0140%.

3.3 Combination A

Combination A involved starved lubrication to the 4140T conformal block on the surface subjected to frictional contact with the D2 ring.

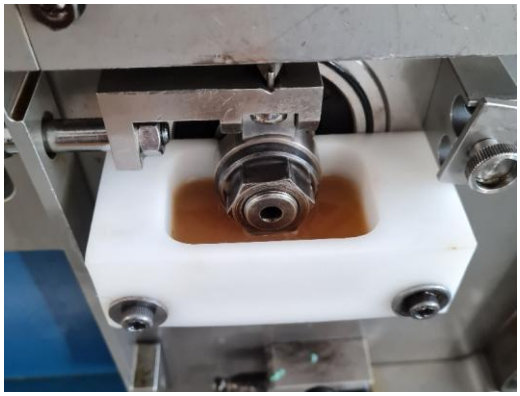

Fig. 6. Starved lubrication condition.

The average displacement increased slowly up to 19.4 µm. The friction force showed a stable behavior, although higher values were observed compared to the dry condition as shown in Fig. 7.

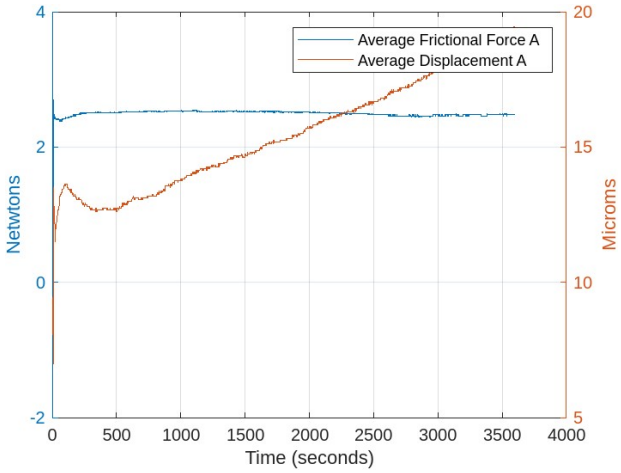

Fig. 7. Average frictional force and displacement versus time for combination A.

The 3D scanning image of one of samples from combination A, shows a more regular surface due to the lubricant layer that reduced the material displacement as shown in Fig. 8.

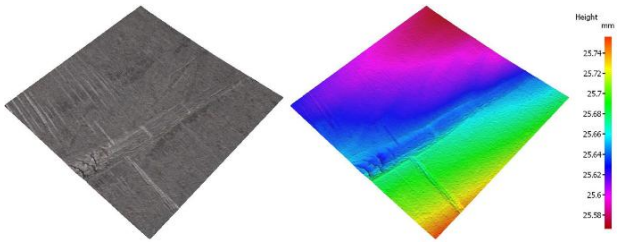

Fig. 8. 3D scanned image of the worn area from a sample of combination A.

The average weight of the samples from combination A before the wear test was 7.4368 grams. After the test, the average weight of the samples was 7.43645 grams and the average material lost was 0.00035 grams. This shows that the average material lost due to frictional contact with starved lubrication was 0.0047%.

3.4 Combination B

Combination B involved LST on the central portion of the concave conformal block surface without lubrication. The maximum average displacement was 72µm and the maximum average frictional force was 6.6 N as shown in Fig. 9.

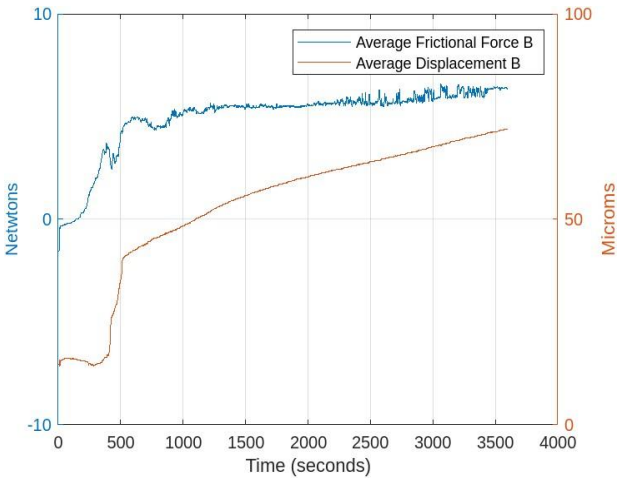

Fig. 9. Average frictional force and displacement versus time for combination B.

The 3D image of one of the samples shows that at the interface in which the LST pattern starts there is displacement of material accumulated compared to the zone of laser marks which appears more uniform as shown in Fig. 10.

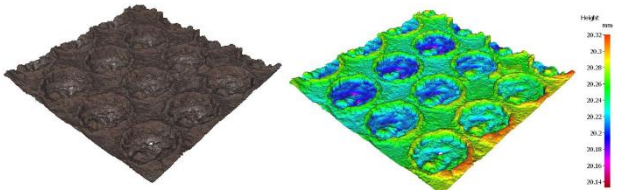

Fig. 10. 3D scanned image of the worn area from a sample of combination B and showing LST surface.

Before the test, the average weight of the samples of the combination B was 8.0311 grams. The average mass of the samples after the test was 8.0299 grams. This shows that the average material weight lost due to frictional contact was 0.0149%.

An important observation is that after the B tests, it was observed debris on the empty lubricant holder as shown in Fig. 11.

Fig. 11. Debris after testing samples from combination B.

3.5 Combination AB

Combination AB involved lubrication and LST. The maximum average displacement was 83 µm. For this combination, it was observed a decreasing behaviour in the frictional force rather than incremental as it was in the case of combinations 1, A, and B as shown in Fig. 12.

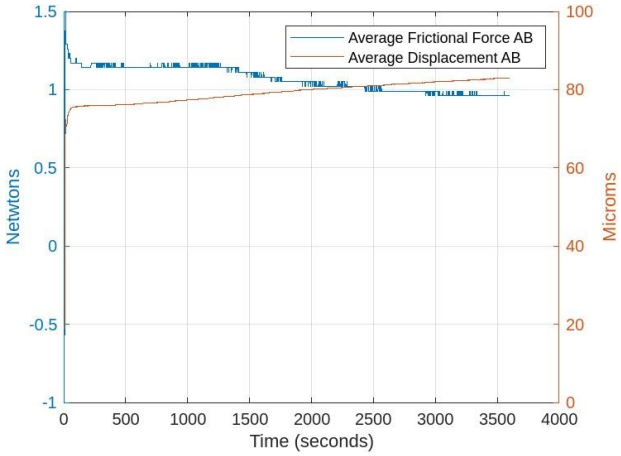

Fig. 12. Average frictional force and displacement versus time for combination AB.

The 3D image of one of the AB samples shows a more regular wear condition, improved surface stability and debris retention as shown in Fig.13.

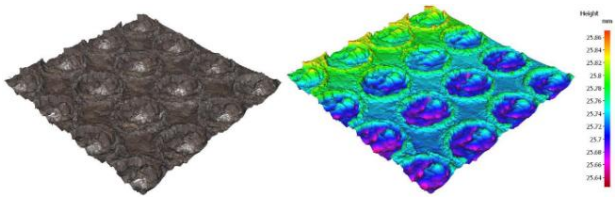

Fig. 13. 3D scanned image of the worn area from a sample of combination AB and showing LST surface.

Additionally, it was observed that the profile is more regular from the transition zone towards the LST zone due to the lower wear-rate as shown in Fig.14.

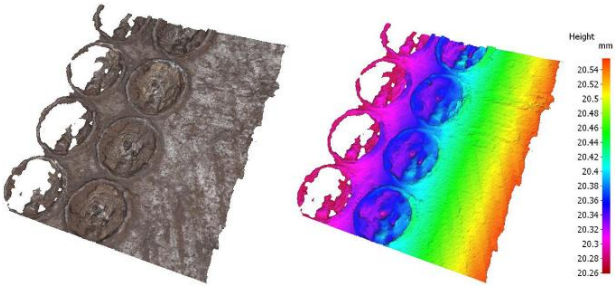

Fig. 14. 3D scanned image of the worn area from a sample of combination AB showing the transition towards the LST area.

Before the test, the average weight of the conformal blocks were 7.0861 grams. After the test, the average weight was 7.0860 grams. This indicates that the average loss of material was 0.0013%.

3.6 Mass loss

The lowest wear was observed under the combined condition (lubrication + LST), while the LST-only condition exhibited higher wear than the dry condition.

Table 4. Percentage of mass lost after the T-05 test for all the combinations.

Combination	% mass lost
1	0.0140%
A	0.0047%
B	0.0149%
AB	0.0013%

As shown in Table 4, the lowest wear was observed in the combined condition (AB), with a mass loss corresponding to 0.0013%. In contrast, the LST-only condition (B) exhibited higher wear than the dry condition.

3.7 Friction behaviour

As shown in Fig. 15, lubricated conditions exhibited more stable friction behavior. The combined condition (AB) showed a decreasing trend in friction over time, indicating improved tribological stability.

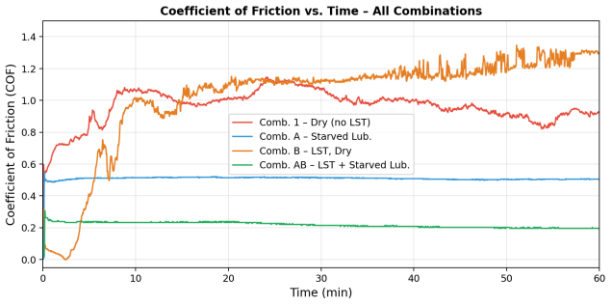

Fig. 15. COF versus time for all combinations.

3.8 Coefficient of Friction behaviour

Fig. 16 shows the average coefficient of friction (COF) for all the combinations. It can be noted that the combination AB provided the smaller average COF with a maximum value of 0.306 and a stable behaviour. Similarly, combination A had a stable behaviour over time and a maximum average COF of 0.551. On the other hand, the rest of the combinations behaved erratically and showed and incremental trend of the COF.

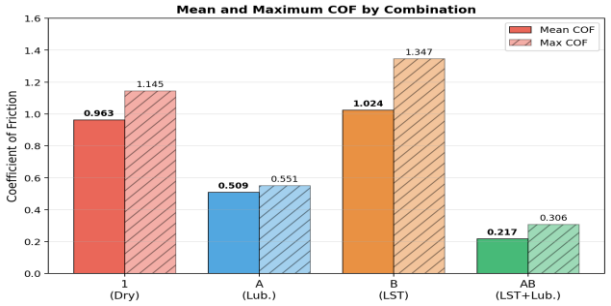

Fig. 16. Mean and maximum COF by combination.

3.9 Surface roughness analysis

Surface profile measurements obtained using the Bruker Alicona optical scanner were performed on selected samples to evaluate the

post-wear surface condition of each combination. Although numerical Ra values were not directly output by the measurement software, the line profile graphs provide qualitative and semi-quantitative evidence of surface roughness after testing.

Fig. 17. Surface zone of combination A used to evaluate profile and roughness.

As shown in Fig.18, the surface profile of Combination A (starved lubrication) showed amplitudes of approximately ±0.5–0.8 µm in the stable wear zone, representing the most homogeneous surface among the non-textured conditions. The border region of the wear scar exhibited amplitudes up to ±3 µm, attributed to displaced material accumulation.

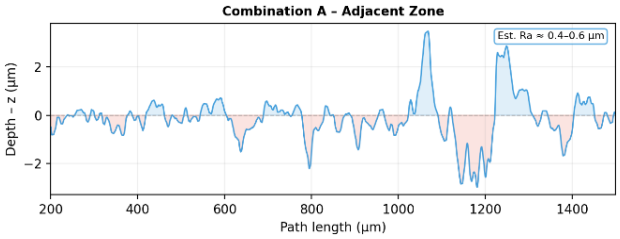

Fig. 18. Surface profile A – Adjacent zone.

As shown in Fig.19, in Combination B (LST, dry), the profile measured within the textured zone showed a regular periodic pattern with amplitudes of approximately ±1.6 µm and a spatial frequency consistent with the texture pitch (~80–100 µm) as shown in Fig.20. In contrast, the non-textured zone of the same sample exhibited irregular amplitudes of ±3–5 µm, indicating severe adhesive wear in areas without surface texturing as shown in Fig.21.

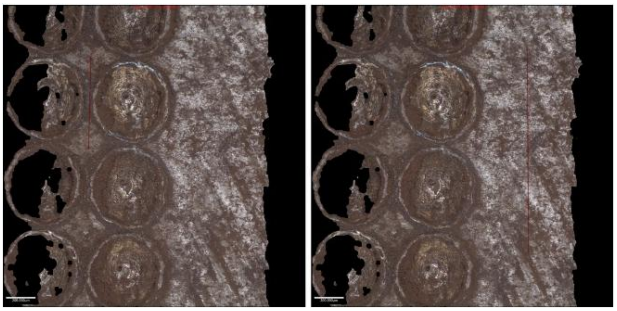

Fig. 19. Surface zone of combination B used to evaluate profile and roughness: LST interface (left) and non LST interface (right).

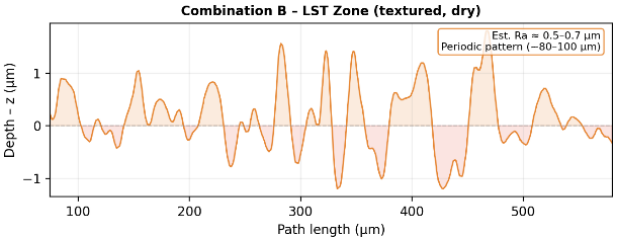

Fig. 20. Surface profile B — LST Zone (periodic pattern ~80–100 µm).

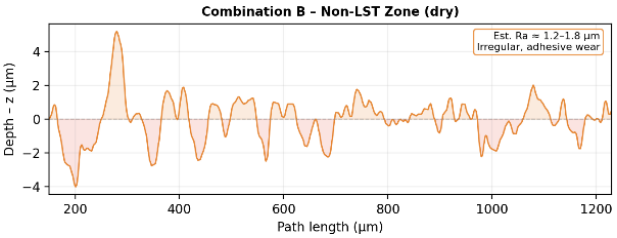

Fig. 21. Surface profile B — Non-LST Zone (roughest surface, adhesive wear).

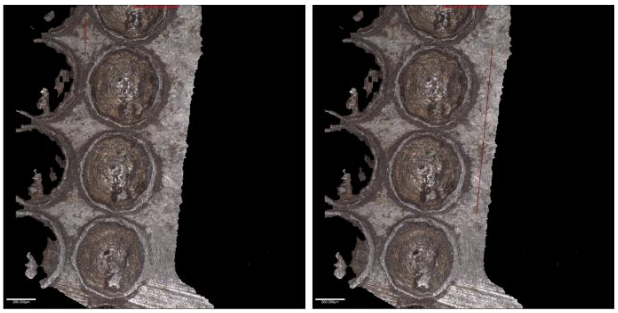

Fig. 22. Surface profile of combination AB used to evaluate profile and roughness: LST interface (left) and non LST interface (right).

Fig.22 shows the Surface profile of combination AB used to evaluate profile and roughness from the LST interface and the non LST interface. The lowest surface roughness was observed in Combination AB (LST + starved lubrication), where the textured zone exhibited profile amplitudes of approximately ±0.9 µm as shown in Fig. 23. This result suggests that the combination

of lubricant retention within the texture features and the reduced contact stress produced the smoothest post-wear surface condition.

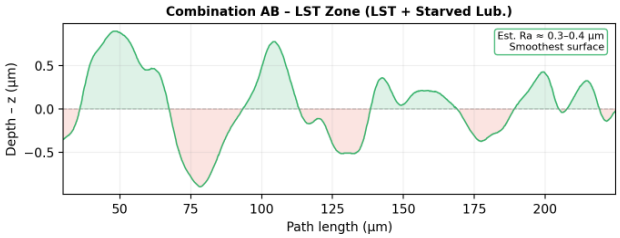

Fig. 23. Surface profile AB — LST Zone (smoothest of all conditions, ~0.3–0.4 µm).

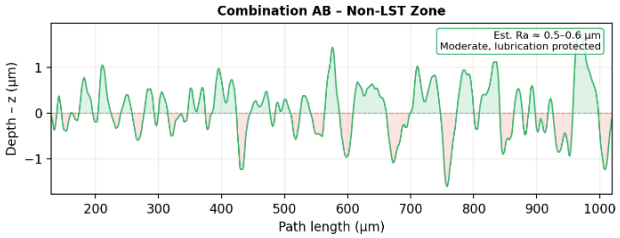

Fig. 24. Surface profile AB — Non-LST Zone (moderate roughness, lubrication-protected).

The non-textured portion of AB samples showed intermediate amplitudes of ±1.5 µm, consistent with partial lubrication protection as shown in Fig. 24.

These observations support the hypothesis that surface texturing under starved lubrication promotes a more stable tribological interface, not only in terms of mass loss but also in terms of resulting surface topography.

The comparatively lower roughness in the LST zones of AB samples may contribute to a self-reinforcing lubrication mechanism, where smoother surfaces facilitate more uniform lubricant film distribution in subsequent contact cycles [5, 7]. Table 5 shows a summary of the roughness surface profile observations.

Table 5. Summary of visual roughness profile observations per combination and measurement zone.

Combination	Zone	Estimated average surface profile (µm)	Observation
A	Stable wear zone	~0.5–0.8	Homogeneous surface
A	Wear scar edge	~2–3	Accumulated displaced material
B	LST zone	~0.5–0.7	Periodic pattern from cavity edges
B	Non-LST zone	~1.2–1.8	Higher roughness, adhesive wear
AB	LST zone	~0.3–0.4	Smoothest surface – synergistic effect
AB	Non-LST zone	~0.5–0.6	Moderate, partially protected by lubricant

3.10 Displacement behaviour

The average and maximum displacement values recorded by the T05 sensor for each combination are presented in Fig. 25. The displacement signal in the T05 system reflects the relative movement of the block holder as wear progresses, providing an indirect indicator of material removal and geometric conformity changes.

Combination A (starved lubrication) exhibited the lowest mean displacement (15.5 µm) and maximum displacement (19.4 µm), consistent with its lowest mass loss and the protective effect of the boundary lubricant film. Combination 1 (dry, no LST) showed intermediate displacement values (mean 22.8 µm, max 31.4 µm), reflecting progressive material removal throughout the test.

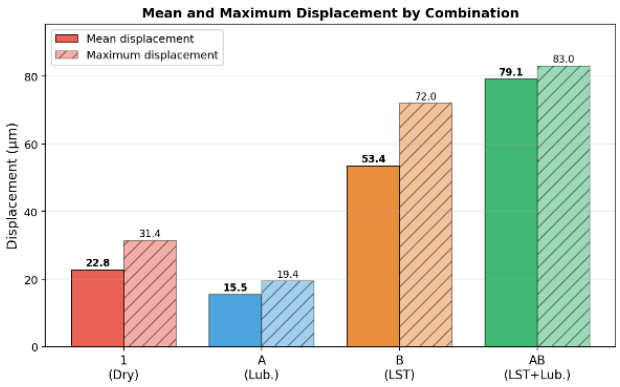

Fig. 25. Mean and maximum displacement by combination.

Combinations B and AB showed higher displacement values (max 72.0 and 83.0 µm respectively). For Combination B, the displacement increased progressively throughout the test duration, consistent with

continuous abrasive wear under dry conditions. In contrast, for Combination AB, analysis of the displacement time series revealed that approximately 54 µm of the total net displacement of 64 µm (measured as the change from initial to final sensor reading: 83 − 18.875 = 64.125 µm) occurred within the first 30 seconds of the test, after which displacement stabilized. This behaviour is attributed to rapid geometric conformity between the textured block surface and the D2 ring, rather than sustained material removal. The subsequent stable displacement rate of Combination AB was the lowest among all combinations, consistent with its superior tribological performance.

This distinction is important: the high total displacement in AB does not contradict its low mass loss. Rather, it indicates that the textured surface underwent rapid geometric seating followed by a stable, low-wear regime enabled by the combined effect of lubricant retention and surface texturing.

3.11 Wear rate analysis

The wear rate was computed as the time derivative of the average displacement signal with respect to time (1), expressed in µm/s as shown in Fig.26. Positive values indicate active material removal events, while zero or negative values reflect sensor noise, elastic recovery, or stable contact phases. This variable provides insight into the dynamics of material removal throughout the test, complementing the cumulative mass loss and displacement measurements.

$$\frac{d\mathcal{F}}{dt} = \frac{\mathcal{F}_2 - \mathcal{F}_1}{t_2 - t_1} \quad (1)$$

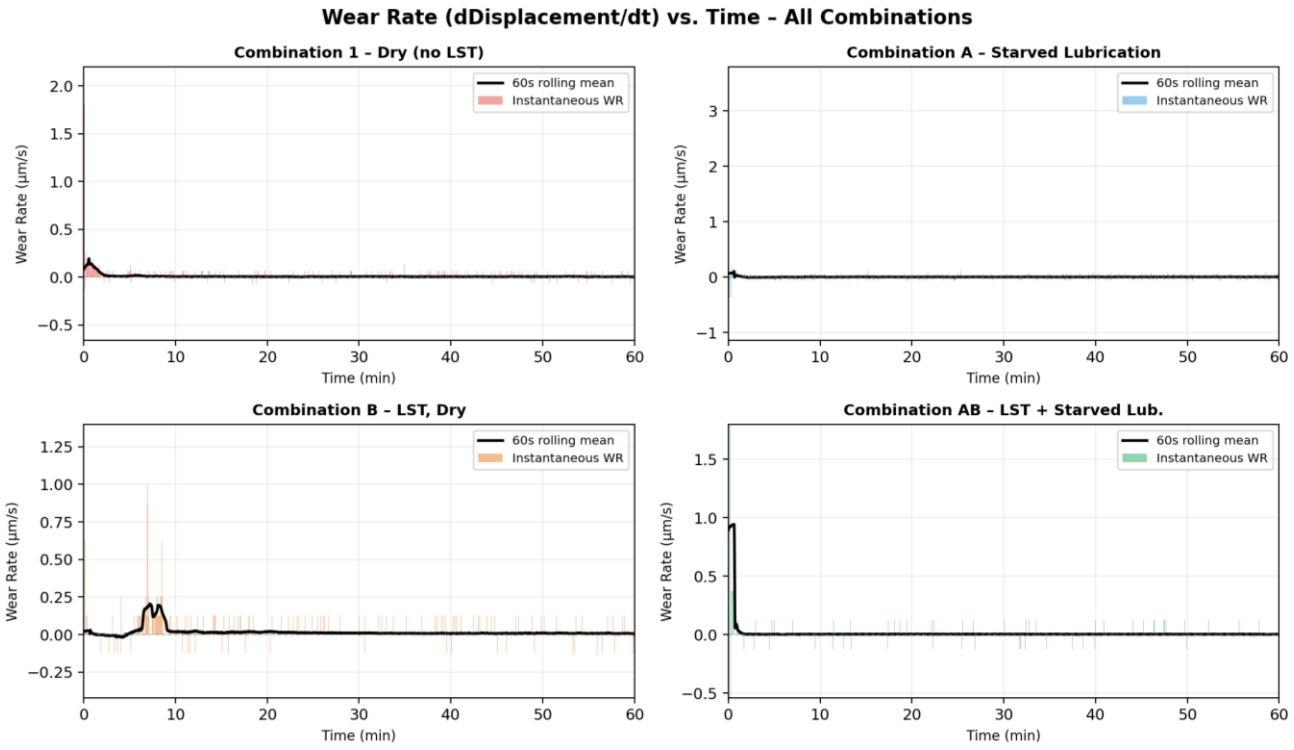

Fig. 26. Wear rate vs. time for all combinations. Bars represent instantaneous values; solid line represents the 60-second rolling mean.

As shown in Fig. 26, the wear rate behaviour differs substantially across combinations. Combination 1 (dry) exhibited a moderate initial wear rate that decayed progressively, reaching a stable level after approximately 10 minutes.

Combination A (starved lubrication) showed the fastest stabilization, with wear activity decreasing to a near-steady state within the first 10 minutes, consistent with rapid formation of a boundary lubricant film.

Combination B (LST, dry) exhibited sustained wear activity throughout the test, with a higher and more persistent rolling mean compared to the lubricated conditions.

Combination AB presented a distinct transient signature: a sharp wear rate peak of 15.5 µm/s occurring between t = 8 and t = 13 s, corresponding to the rapid geometric conformity phase identified in the displacement analysis.

Following this initial phase, the wear rate dropped immediately to the lowest sustained level among all combinations, confirming that the apparent high displacement in AB is attributable to initial seating rather than progressive material removal as shown in Fig. 27.

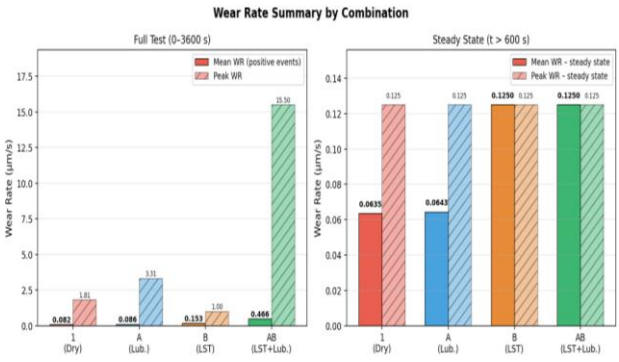

Fig. 27. Wear rate summary by combination: mean and peak values for the full test (left) and steady-state phase (right, t > 600 s).

Fig. 27 presents the mean and peak wear rate values for each combination under full-test and steady-state conditions, computed over active wear events (WR>0). During the full test, the mean positive wear rate of Combination AB appears elevated (0.466 µm/s) due to the brief but intense initial seating event.

In contrast, the steady-state mean wear rate of AB (0.125 µm/s) is identical to that of Combination B, indicating that once geometric conformity is achieved, both textured conditions produce the same instantaneous wear rate magnitude during active events.

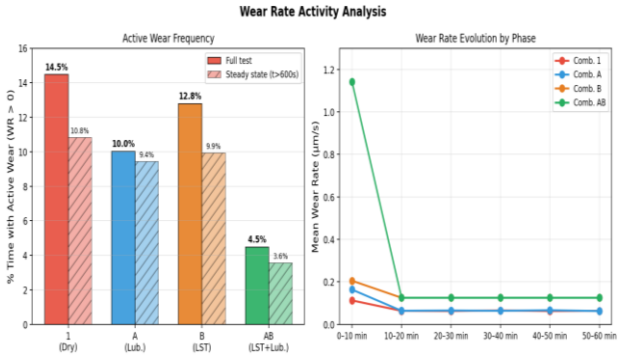

Fig. 28. Active wear frequency (left) and wear rate evolution by 10-minute phase (right).

Notably, Combinations 1 and A converge to nearly identical steady-state mean wear rates (0.0635 and 0.0643 µm/s respectively), suggesting that the dominant factor distinguishing their total wear is not the magnitude of individual wear events but their frequency — as confirmed by the active wear frequency analysis as shown in Fig. 28.

Fig. 28 reveals that Combination AB exhibited active wear (WR > 0) during only 4.5% of the total test duration (3.6% in steady state), compared to 14.5% for Combination 1, 10.0% for A, and 12.8% for B. This represents a reduction of approximately 67% in active wear time relative to the dry condition during steady state. The phase evolution plot (right) confirms that all combinations converge toward similar instantaneous wear rate levels after the first 10 minutes, and that the key differentiator of AB is the dramatically reduced frequency of wear events rather than a lower per-event magnitude.

These findings provide a mechanistic interpretation for the superior tribological performance of Combination AB: the surface texture features retain lubricant that interrupts metal-to-metal contact repeatedly throughout the test, effectively reducing the proportion of time during which active material removal occurs. This mechanism operates independently of the instantaneous wear rate, which converges to similar values across textured conditions in steady state.

4. DISCUSSION

The results indicate that starved lubrication reduces wear by limiting direct asperity interaction and promoting boundary film formation [2].

Laser surface texturing enhances this effect by acting as a reservoir for lubricant retention and as a trap for wear debris, reducing third-body abrasion [3, 4, 13].

As shown in Fig. 13, the combined condition (AB) exhibited reduced mass loss and a more stable wear profile, which is consistent with the improved lubricant retention observed in the textured regions.

The observations presented in Fig. 10 and Fig. 13 support the hypothesis that larger texture features promote localized retention of lubricant and wear debris, contributing to improved tribological performance under starved lubrication conditions.

Unlike conventional approaches favoring smaller texture diameters [3, 4], this study employed larger circular features to increase volumetric capacity. Under the tested starved lubrication conditions, this approach appears to improve local lubricant availability and debris retention.

These observations suggest that, under boundary lubrication regimes, the volumetric capacity of surface textures may be more relevant than texture density alone. However, this conclusion is exploratory and requires further validation.

The increased wear observed in the LST-only condition may be attributed to surface modification effects induced during laser processing, leading to increased susceptibility to abrasive wear [13].

Water-based emulsified fluids similar to the one used in this study are widely applied in industrial operations beyond machining, including forming, grinding, and surface finishing processes [9].

The combined condition demonstrated improved performance, indicating a potential synergistic interaction between lubrication and surface texturing [13, 14]. Therefore, the observed behaviour under starved lubrication conditions may be relevant to a broader range of tribological systems where limited lubricant supply is present.

This study contributes exploratory evidence on the combined effect of LST and starved lubrication on 4140/D2 steel interfaces, using larger texture diameters than typically reported.

4.1 Limitations of the study

Despite the consistency of the observed trends, this study presents several limitations:

- Limited replication was performed due to limited time and resources available at the time of data collection.
- Statistical analysis could not be performed.
- SEM imaging and volumetric wear measurements were not available.

These limitations do not invalidate the findings but restrict their generalizability. Therefore, the results should be interpreted as exploratory trends.

Future work should include, besides a statistical analyses, profilometry-based volume loss measurements and SEM analysis to identify dominant wear mechanisms.

5. CONCLUSION

- Starved lubrication reduces wear compared to dry conditions.
- Laser surface texturing alone may increase wear under dry conditions.
- The combination of lubrication and LST shows the lowest wear.
- Surface observations confirm improved lubricant retention and debris trapping.
- Larger texture diameters may enhance tribological performance under starved lubrication conditions.
- The LST zone in Combination AB exhibited the lowest post-wear surface roughness (~±0.9 μm profile amplitude), suggesting that surface texturing under starved lubrication promotes a more stable tribological interface and smoother contact surface.
- Under dry conditions (Combination B), the non-textured zone adjacent to the LST pattern showed greater surface irregularity (±3–5 μm) than the textured zone (±1.6 μm), indicating that surface texturing provides localized protection even without lubrication.
- The displacement analysis reveals that the high total displacement in Combination AB is primarily attributable to rapid geometric conformity during the initial phase of testing (~57 μm in the first 30 s), followed by the lowest sustained wear rate among all combinations. This behavior distinguishes geometric seating from material removal.
- The combined condition (AB) exhibited active material removal during only 3.6% of the steady-state test duration, compared to 10.8%, 9.4%, and 9.9% for combinations 1, A, and B respectively, indicating that the primary wear-reduction mechanism of LST under starved lubrication is a reduction in contact frequency rather than a reduction in instantaneous wear rate.
- In steady state, the instantaneous wear rate during active events converges to similar values across conditions that include surface texturing (B and AB: 0.125 μm/s), while non-textured conditions (1 and A) settle at approximately half that value (0.064 μm/s). This suggests that textured surfaces experience more energetic individual wear events, but far less frequently.

- The wear rate phase evolution confirms that all combinations reach a tribological steady state after approximately 10 minutes of testing, after which wear dynamics remain stable for the remainder of the 60-minute test duration.

These findings suggest a potential synergistic effect between lubrication and surface texturing, particularly when texture design prioritizes volumetric capacity and contributes to the understanding of surface texturing design under constrained lubrication regimes.

Acknowledgement

The author gratefully acknowledges the University of Monterrey for providing access to laboratory facilities and experimental equipment that made this study possible during the course of the author's master's studies. The author also acknowledges a Tier 1 automotive supplier located in Monterrey, Nuevo Leon, Mexico, for kindly providing the AISI 4140 steel block samples and the water-based cutting fluid used in this study. Finally, the author acknowledges that Generative AI, Claude (Anthropic, claude-sonnet 4.6) was used only to assist with language editing and improvement, as well as for literature search and classification purposes.

REFERENCES

[1] S. Kalpakjian, *Manufacturing Engineering and Technology*, 7th ed. Boston, MA, USA: Addison-Wesley, 2015, pp. 144–154.

[2] G. W. Stachowiak and A. W. Batchelor, *Engineering Tribology*, 4th ed. Oxford, U.K.: Butterworth-Heinemann, 2014, ch. 8, pp. 367–420.

[3] J. L. Guo, T. Hu, Q. Li, and Y. H. Liu, "Nanosecond laser-induced dimple texturing of TB6 alloy surfaces: Tribological behavior under dry and starved-oil lubrication," *Tribology International*, vol. 197, p. 109842, 2024, doi: 10.1016/j.triboint.2024.109842.

[4] D. Kumar, J. Daniel, and S. K. Biswas, "Tribology of steel/steel interaction in oil-in-water emulsion: A rationale for lubricity," *Journal of Colloid and Interface Science*, vol. 345, no. 2, pp. 307–315, 2010, doi: 10.1016/j.jcis.2010.01.068.

[5] R. S. Long, Q. Y. Shang, Z. H. Jin, Y. M. Zhang, Z. C. Ju, and M. H. Li, "Tribological behavior of laser textured rolling element bearings under starved lubrication," *Industrial Lubrication and Tribology*, vol. 74, no. 5, pp. 453–462, 2022, doi: 10.1108/ILT-10-2021-0420.

[6] L. Peña-Parás, D. Maldonado-Cortés, M. Rodríguez-Villalobos, A. G. Romero-Cantú, and O. E. Montemayor, "Enhancing tool life and reducing power consumption and surface roughness in milling processes by nanolubricants and laser surface texturing," *Journal of Cleaner Production*, vol. 253, p. 119836, 2020, doi: 10.1016/j.jclepro.2019.119836.

[7] D. Maldonado-Cortés, L. Peña-Parás, V. Barrios Saldaña, J. S. Cruz-Bañuelos, and M. Adamiak, "Synergistic effect on the tribological properties of tool steel through the use of laser surface texturing channels and nanoparticles," *Wear*, vol. 426–427, pp. 1354–1361, 2019, doi: 10.1016/j.wear.2019.01.040.

[8] ASTM G77-05, *Standard Test Method for Ranking Resistance of Materials to Sliding Wear Using Block-on-Ring Wear Test*, ASTM International, 2005.

[9] I. Etsion, "State of the art in laser surface texturing," *Journal of Tribology*, vol. 127, no. 1, pp. 248–253, 2005, doi: 10.1115/1.1828070.

[10] Y. Xu *et al.*, "Influence of dimple shape on tribofilm formation and tribological properties of textured surfaces under full and starved lubrication," *Tribology International*, vol. 136, pp. 267–275, 2019, doi: 10.1016/j.triboint.2019.03.047.

[11] A. Rosenkranz, P. G. Grützmacher, C. Gachot, and L. Costa, "Surface texturing in machine elements—a critical discussion for rolling and sliding contacts," *Advanced Engineering Materials*, vol. 21, no. 8, p. 1900194, 2019, doi: 10.1002/adem.201900194.

[12] J. Ma, Y. Liu, and J. Mostaghimi, "Effect of laser preparation strategy on surface wettability and tribological properties under starved lubrication," *Tribology International*, vol. 191, p. 109107, 2024, doi: 10.1016/j.triboint.2023.109107.

[13] R. Meng, J. Deng, and R. Duan, "Modifying tribological performances of AISI 316 stainless steel surfaces by laser surface texturing and various solid lubricants," *Optics and Laser Technology*, vol. 109, pp. 401–411, 2019, doi: 10.1016/j.optlastec.2018.08.020.

[14] Z. Wang, R. Ye, and J. Xiang, "The performance of textured surface in friction reduction: A review," *Tribology International*, vol. 177, p. 108010, 2023, doi: 10.1016/j.triboint.2022.108010.